Kinetic Analysis of Translesion Synthesis Opposite Bulky N^2- and O^6-Alkylguanine DNA Adducts by Human DNA Polymerase REV1*[S]

Jeong-Yun Choi[‡1] **and F. Peter Guengerich**[§]

From the ‡*Department of Pharmacology, School of Medicine, Ewha Womans University, 911-1, Mok-6-dong, Yangcheon-gu, Seoul 158-710, Republic of Korea and the* §*Department of Biochemistry and Center in Molecular Toxicology, Vanderbilt University School of Medicine, Nashville, Tennessee 37232-0146*

REV1, a Y family DNA polymerase (pol), is involved in replicative bypass past DNA lesions, so-called translesion DNA synthesis. In addition to a structural role as a scaffold protein, REV1 has been proposed to play a catalytic role as a dCTP transferase in translesion DNA synthesis past abasic and guanine lesions in eukaryotes. To better understand the catalytic function of REV1 in guanine lesion bypass, purified recombinant human REV1 was studied with two series of guanine lesions, N^2-alkylG adducts (in oligonucleotides) ranging in size from methyl (Me) to CH_2(6-benzo[a]pyrenyl) (BP) and O^6-alkylG adducts ranging from Me to 4-oxo-4-(3-pyridyl)butyl (Pob). REV1 readily produced 1-base incorporation opposite G and all G adducts except for O^6-PobG, which caused almost complete blockage. Steady-state kinetic parameters (k_{cat}/K_m) were similar for insertion of dCTP opposite G and N^2-G adducts but were severely reduced opposite the O^6-G adducts. REV1 showed apparent pre-steady-state burst kinetics for dCTP incorporation only opposite N^2-BPG and little, if any, opposite G, N^2-benzyl (Bz)G, or O^6-BzG. The maximal polymerization rate (k_{pol} 0.9 s^{-1}) opposite N^2-BPG was almost the same as opposite G, with only slightly decreased binding affinity to dCTP (2.5-fold). REV1 bound N^2-BPG-adducted DNA 3-fold more tightly than unmodified G-containing DNA. These results and the lack of an elemental effect ((S_p)-2'-deoxycytidine 5'-O-(1-thiotriphosphate)) suggest that the late steps after product formation (possibly product release) become rate-limiting in catalysis opposite N^2-BPG. We conclude that human REV1, apparently the slowest Y family polymerase, is kinetically highly tolerant to N^2-adduct at G but not to O^6-adducts.

Cellular DNA is continuously attacked by various endogenous and exogenous agents. Although the resulting lesions can be removed by versatile cellular repair systems, many DNA lesions escape repair and are usually present in replicating DNA. Facing DNA lesions during DNA replication, DNA polymerases often show unusual behavior, such as misinsertion, slippage, and blockage, which can give rise to mutations or cell death (1). Therefore, the characterization of interaction of DNA polymerases with DNA lesions is crucial for understanding the mechanism of mutagenesis in cells in detail (2). Human cells possess at least 15 different DNA polymerases, the physiological functions of most of which are still unclear. Replicative DNA polymerases, such as pol[2] α, δ, and ϵ, are intolerant of DNA distortions caused by many DNA lesions and thus are blocked (3). As a tolerance mechanism to this replication blockade, cells utilize the specialized translesion synthesis (TLS) DNA polymerases, which have a spacious active site to replicate past replication fork-blocking lesions (4). Many of human TLS DNA polymerases belong to the recently discovered Y family, including pol η, pol ι, pol κ, and REV1 (5). Y family members often have different properties of bypass ability and fidelity opposite various DNA lesions (4).

The N2 and O6 atoms at G are highly susceptible to modification by various potential carcinogens. The N2 atom of G is easily modified by formaldehyde (6), acetaldehyde (7), and the oxidation products of heterocyclic amines (*e.g.* 2-amino-3-methylimidazo[4,5-f]quinoline (8)) and polycyclic aromatic hydrocarbons (*e.g.* benzo[a]pyrene (9)), forming various N^2-G derivatives, such as Me, Et, 2-amino-3-methylimidazo[4,5-f]quinoline, and benzo[a]pyrene diol epoxide adducts. In a different way, the O6 atom of G is readily modified by DNA-alkylating agents (10, 11) and metabolites of tobacco-specific carcinogen 4-(methylnitrosoamino)-1-(3-pyridyl)-1-butanone (12), forming various O^6-G adducts, such as Me, Et, and 4-oxo-4-(3-pyridyl)butyl (Pob) adducts. Relatively large G adducts, such as N^2-benzo[a]pyrene diol epoxide-G (13) and O^6-PobG (14) produce mutations in bacterial and mammalian cells. Even small G adducts, such as N^2-EtG and O^6-EtG, also produce some mutations in bacterial and human cells (15, 16) but with varied spectra and frequencies. These diverse mutagenicities of

G lesions may be attributable to the differences in translesion DNA synthesis for each. To better understand TLS processes at N^2- and O^6-G lesions and the mechanisms of mutagenesis, we have previously addressed the details of lesion bypass across various N^2-G and O^6-G adducts by DNA polymerases, including replicative polymerases, such as human immunodeficiency virus type 1 reverse transcriptase, pol T7⁻ (17–19), and human pol δ and TLS polymerases, such as human pol η, ι, and κ (20–25).

REV1, a Y family polymerase, is believed to play both structural and catalytic roles in TLS in eukaryotes. REV1 has been suggested to serve as a scaffold protein for the recruitment of polymerases by the ability of interactions with proteins PCNA (26), ubiquitinated proteins (27), and polymerases η, ι, κ, and ζ (28). In its catalytic role as a polymerase, REV1 can catalyze the preferential insertion of dCTP opposite template G, apurinic/apyrimidinic sites, and the various damaged bases (29–33) by utilizing a unique mechanism of protein-template-directed nucleotide incorporation (34), but the enzymatic role of REV1 in TLS still remains to be elucidated. With a unique ability for selective dCTP insertion, REV1 inherently has the potential to play a role in error-free bypass opposite guanine DNA lesions. Although the suggestion has been advanced that REV1 can incorporate dCTP opposite some minor groove guanine adducts and facilitate the lesion bypass (35), quantitative evidence to support this suggestion is still limited.

In order to obtain a better understanding of the catalytic role of human REV1 in bypass of guanine lesions, we performed steady-state and pre-steady-state kinetic studies with this enzyme and site-specifically modified oligonucleotides containing various N^2-G and O^6-G adducts. The results obtained with REV1 can also be compared with the corresponding studies done with three other human Y family polymerases, pol η (22), pol ι (21), and pol κ (20). Our results indicate that REV1 catalysis is remarkably resistant to the large lesions at guanine N2, very similar to pol κ, but not at guanine O6. This study also provides detailed kinetic information on human REV1, which is quite different from other human Y family polymerases.

EXPERIMENTAL PROCEDURES

Materials—Unlabeled dNTPs, T4 polynucleotide kinase, and restriction endonucleases were purchased from New England Biolabs (Ipswich, MA). (S_p)-dCTPαS was purchased from Biolog Life Science Institute (Bremen, Germany). [γ-³²P]ATP (specific activity 3,000 Ci/mmol) was purchased from PerkinElmer Life Sciences. Bio-spin columns were purchased from Bio-Rad. A protease inhibitor mixture was obtained from Roche Applied Science. Human testis cDNA was purchased from BD Biosciences Clontech. *Pfu Ultra* DNA polymerase and pPCR-Script Amp vector were purchased from Stratagene (La Jolla, CA). Amicon Ultra centrifugal filter devices were purchased from Millipore (Billerica, MA).

Oligonucleotides—Unmodified 24- and 36-mer (Table 1) were purchased from Midland Certified Reagent Co. (Midland, TX). Eleven 36-mers, each containing a guanine N^2- or O^6-adduct (N^2-MeG, N^2-EtG, N^2,N^2-diMeG, N^2-IbG, N^2-BzG, N^2-NaphG, N^2-AnthG, N^2-BPG, O^6-MeG, O^6-BzG, and O^6-PobG) were prepared as previously described (17, 21–23).

TABLE 1
Oligodeoxynucleotides used in this study

Oligodeoxynucleotide	Sequence
24-mer	5′GCCTCGAGCCAGCCGCAGACGCAG
25-mer	5′GCCTCGAGCCAGCCGCAGACGCAGC
36-mer[a]	3′CGGAGCTCGGTCGGCGTCTGCGTC**G***CTC CTGCGGCT

[a] **G***=G, N^2-MeG, N^2-EtG, N^2-IbG, N^2-BzG, N^2-NaphG, N^2-AnthG, N^2-BPG, N^2,N^2-diMeG, O^6-MeG, O^6-BzG, or O^6-PobG.

The extinction coefficients for the oligonucleotides, estimated by the Borer method (36), were as follows: 24-mer, $\epsilon_{260} = 224$ mM⁻¹ cm⁻¹; 36-mer, $\epsilon_{260} = 310$ mM⁻¹ cm⁻¹.

Isolation of Human REV1 cDNA and Construction of Escherichia coli Expression Vector—The human *REV1* cDNA was obtained as two overlapping cDNA fragments by PCR amplifications (the 2.2-kb coding region from the 5′-end and the 1.8-kb coding region from the 3′-end) from human testis cDNAs (as template) using *Pfu Ultra* DNA polymerase with the two sets of corresponding primers (5′-CATATGCATC-ACCATCACCATCACATGAGGCGAGGTGGATGG-3′ and 5′-CTTCTGCCTCTTTTGGCTGAGT-3′ for the 5′-end coding region of *REV1*; 5′-TTGTGGAGACTTGCAGTA-3′ and 5′-CTCGAGTTATGTAACTTTTAATGTGC-3′ for the 3′-end coding region of *REV1*). The resulting 2.2- and 1.8-kb PCR products of *REV1* were cloned into the vector pPCR-Script Amp, respectively, and nucleotide sequencing was used to confirm the sequence of the coding region. The full-length human *REV1* cDNA was constructed by ligating a 2.1-kb SmaI/BstBI fragment containing the 5′-fragment of *hREV1* into the SmaI/BstBI sites of the 4.6-kb pPCR-Script Amp vector containing 3′-fragment of *hREV1*. The 3.8-kb human *REV1* cDNA fragment was then cloned into the NdeI and XhoI sites of the vector pET-22b(+), generating pET22b(+)/hREV1-NHis6 vector.

Expression and Purification of Human REV1—Recombinant human REV1, fused to an N-terminal His₆ tag, was expressed in *E. coli* strain BL21(DE3). *E. coli* BL21(DE3) harboring the vector (24 liters) was grown in Luria-Bertani broth supplemented with ampicillin (100 μg ml⁻¹) at 25 °C, with aeration, to A_{600} 0.6. Isopropyl-β-D-thiogalactopyranoside was added to 0.2 mM, and the incubation was continued for 11 h at 15 °C. The cells were harvested by centrifugation and resuspended in 60 ml of lysis buffer (50 mM Tris-HCl, pH 7.4, containing 300 mM NaCl, 10% glycerol (v/v), 5 mM β-mercaptoethanol, 1 mg/ml lysozyme, and protease inhibitor mixture (Roche Applied Sciences), cooled on ice for 30 min, and then lysed by sonication (12 × 10 s duration with a Branson digital sonifier (VWR, West Chester, PA), microtip, 45% amplitude, with intervening cooling time). The cell lysate was clarified by centrifugation at $4 \times 10^4 \times g$ for 60 min at 4 °C. The resulting supernatant was loaded (0.3 ml min⁻¹) onto a 5-ml size FPLC HisTrap HP column (Amersham Biosciences) at 4 °C. The column was washed (at 0.8 ml min⁻¹) with 50 ml of Buffer A (50 mM Tris-HCl, pH 7.5, with 500 mM NaCl, 10% glycerol (v/v), and 5 mM 2-mercaptoethanol) containing 20 mM imidazole, 50 ml of Buffer A containing 40 mM imidazole, and then with 50 ml of Buffer A containing 50 mM imidazole. Bound His₆-tagged REV1 was eluted with 400 mM imidazole in Buffer B. Fractions containing REV1 were collected and diluted 2-fold with Buffer B (50 mM Tris-

HCl (pH 7.5) containing 10% glycerol (v/v), 5 mM 2-mercapto-ethanol, and 1 mM EDTA) and loaded onto a Mono Q column (Amersham Biosciences Bioscience). REV1 was eluted with a 50-ml linear gradient of 250 mM to 1 M NaCl in Buffer B. Eluted fractions (0.26 ml) were analyzed by SDS-polyacrylamide gel electrophoresis, and REV1 was found to be eluted at 320 mM NaCl. Fractions containing REV1 were collected and loaded onto a HiTrap Heparin HP column (Amersham Biosciences Bioscience). REV1 was eluted with a 50-ml linear gradient of 400 mM to 1 M NaCl in Buffer B. Eluted fractions (0.26 ml) were analyzed by SDS-polyacrylamide gel electrophoresis, and REV1 was found to be eluted at 700 mM NaCl. The pooled fractions containing REV1 were concentrated (using an Amicon Ultra centrifugal filter; Millipore) to a volume of 100 μl and further purified using a Superdex 200 column (Amersham Biosciences) with buffer B containing 400 mM NaCl. Fractions containing recombinant protein were pooled, concentrated, and exchanged into storage buffer (50 mM Tris-HCl, pH 7.5, containing 50% glycerol (v/v), 5 mM 2-mercaptoethanol, 1 mM EDTA, and 400 mM NaCl). The yield was about 330 μg from 24 liters of culture. The protein concentration was determined using a calculated ϵ_{280} value of 102 mM^{-1} cm^{-1} for REV1 (37). An SDS-polyacrylamide gel electrophoretogram of purified REV1 is included in Fig. S1.

Reaction Conditions for Enzyme Assays—Unless indicated otherwise, standard DNA polymerase reactions were performed in 50 mM Tris-HCl (pH 7.5) buffer containing 50 mM NaCl, 5 mM dithiothreitol, 100 μg ml^{-1} bovine serum albumin (w/v), and 10% glycerol (v/v) with 100 nM primer-template at 37 °C. Primers were 5′-end-labeled using T4 polynucleotide kinase with [γ-^{32}P]ATP and annealed with template (36-mer). All reactions were initiated by the addition of dNTP and MgCl$_2$ (5 mM final concentration) to preincubated enzyme/DNA mixtures.

Primer Extension Assay with All Four dNTPs—A ^{32}P-labeled primer, annealed to either an unmodified or adducted template, was extended in the presence of all four dNTPs (100 μM each) for 15 min. Reaction mixtures (8 μl) were quenched with 2 volumes of a solution of 20 mM EDTA in 95% formamide (v/v). Products were resolved using a 16% polyacrylamide (w/v) gel electrophoresis system containing 8 M urea and visualized using a Bio-Rad Molecular Imager FX and Quantity One software (Bio-Rad).

Steady-state Reactions—A ^{32}P-labeled primer, annealed to either an unmodified or adducted template, was extended in the presence of increasing concentrations of a single dNTP. The molar ratio of primer/template to enzyme was at least 10:1, except for dGTP, dTTP, and O^6-PobG-adducted template. Enzyme concentrations and reaction times were chosen so that maximal product formation would be $\leq$20% of the substrate concentration (38). The primer-template was extended with dNTP in the presence of 0.1–50 nM enzyme for 5 or 10 min. All reactions (8 μl) were done at 10 dNTP concentrations and quenched with 10 volumes of a solution of 20 mM EDTA in 95% formamide (v/v). Products were resolved using a 16% polyacrylamide (w/v) electrophoresis gel containing 8 M urea and quantitated by phosphorimaging analysis using a Bio-Rad molecular imager FX instrument and Quantity One software.

Graphs of product formation *versus* dNTP concentration were fit using nonlinear regression (hyperbolic fits) in GraphPad Prism (San Diego, CA) for the determination of k_{cat} and K_m values.

Pre-steady-state Reactions—Rapid quench experiments were performed using a model RQF-3 KinTek Quench Flow Apparatus (KinTek Corp., Austin, TX). Reactions were initiated by rapid mixing of ^{32}P-primer/template/polymerase mixtures (12.5 μl) with the dNTP-Mg^{2+} complex (10.9 μl) and then quenched with 0.3 M EDTA after times varying from 5 ms to 15 s for N^2-BzG-, O^6-BzG-, N^2-BPG-, and O^6-PobG-containing DNA. Reactions were mixed with 450 μl of formamide-dye solution (20 mM EDTA, 95% formamide (v/v), 0.5% bromphenol blue (w/v), and 0.05% xylene cyanol (w/v)) and run on a denaturing electrophoresis gel, with quantitation as described for the steady-state reactions. Pre-steady-state experiments were fit with the burst equation $y = A(1 - e^{-kpt}) + k_{ss}t$, where y = concentration of product, A = burst amplitude, k_p = pre-steady-state rate of nucleotide incorporation, t = time, and k_{ss} = steady-state rate of nucleotide incorporation (not normalized for enzyme concentration in the equation) (39, 40), using nonlinear regression analysis in GraphPad Prism software. Results obtained under single turnover conditions were fit with the burst equation $y = A(1 - e^{-kpt})$ (see above).

Phosphorothioate Analysis—With the ^{32}P-primer annealed to an N^2-BPG-adducted template, reactions were initiated by rapid mixing of ^{32}P-primer/template/polymerase mixtures (12.5 μl) with an (S_p)-dCTPαS-Mg^{2+} complex (or dCTP-Mg^{2+}) (10.9 μl) and then quenched with 0.3 M EDTA after reaction times varying from 5 ms to 30 s. Products were analyzed as described for the pre-steady-state reactions mentioned earlier.

Determination of K_d^{dCTP}—K_d^{dCTP} was estimated by performing pre-steady-state reactions at different dNTP concentrations with reaction times varying from 5 ms to 15 s. A graph of the burst rate (k_{obs}) *versus* dCTP concentration was fit to the hyperbolic equation $k_{obs} = k_{pol}[dNTP]/([dNTP] + K_d)$, where k_{pol} is the maximal rate of nucleotide incorporation, and K_d^{dCTP} is the equilibrium dissociation constant for dCTP (39, 40).

Estimation of the Apparent Dissociation Constant (K_d) for DNA by Electrophoretic Mobility Shift Assay—Increasing concentrations of human REV1 (2.5–320 nM) were incubated with 0.5 nM ^{32}P-labeled 24-mer/36-mer primer-template DNA on ice for 15 min in the binding buffer containing 50 mM Tris-HCl (pH 8.0 at 4 °C), 50 mM NaCl, 50 mM MgCl$_2$, 5 mM dithiothreitol, 100 μg ml^{-1} bovine serum albumin (w/v), and 10% glycerol (v/v). The mixtures were directly loaded on nondenaturing 4% polyacrylamide gels and electrophoresed at 8 V cm^{-1} for 1 h at 4 °C in the running buffer (40 mM Tris acetate (pH 8.0 at 4 °C) containing 5 mM magnesium acetate and 0.1 mM EDTA. The fractions of REV1-bound DNA were quantitated using a Bio-Rad molecular imager FX instrument and Quantity One software. Assuming a 1:1 stoichiometry between REV1 and DNA substrate, the data were fit to a single-site binding equation (41), $\theta = [E_f]/(K_d + [E_f])$, where θ = fraction saturation and $[E_f]$ = free enzyme concentration, in GraphPad Prism software. The free enzyme concentration was estimated using a conservation of
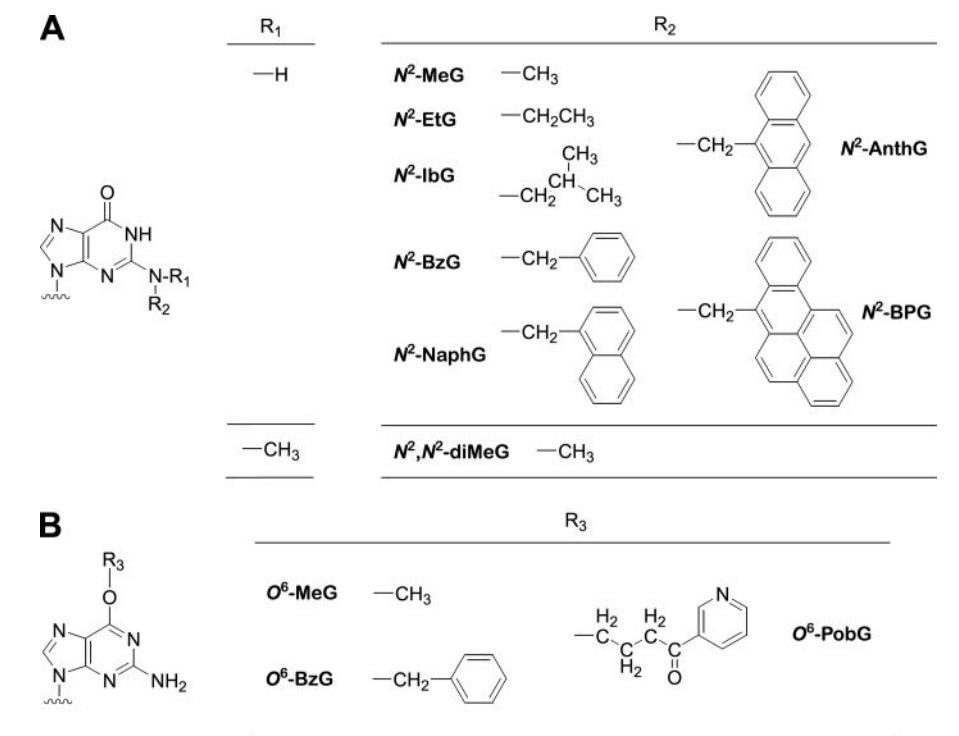
FIGURE 1. **Guanine DNA adducts used in this work.** *A*, N^2-guanine derivatives; *B*, O^6-guanine derivatives.
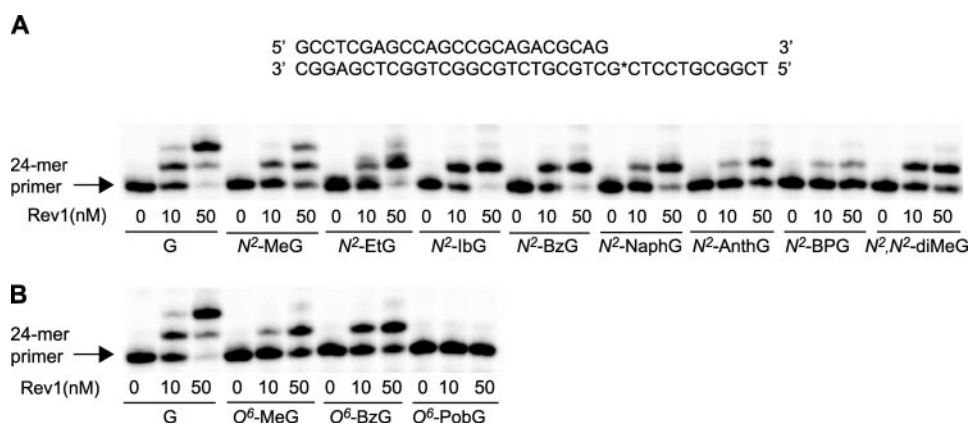

FIGURE 2. **Extension of ^{32}P-labeled primers opposite G and N^2- and O^6-G adducts by human REV1 in the presence of all four dNTPs.** *A*, opposite G, N^2-MeG, N^2-EtG, N^2-IbG, N^2-BzG, N^2-NaphG, N^2-AnthG, N^2-BPG, and N^2,N^2-diMeG; *B*, opposite G, O^6-MeG, O^6-BzG, and O^6-PobG. Primer (24-mer) was annealed with each of the 12 different 36-mer templates (Table 1) containing an unmodified G or N^2- or O^6-modified G placed at the 25th position from the 3′-end (see Fig. 1). Reactions were performed for 15 min with increasing concentrations of REV1 (0–50 nM) and a constant concentration of DNA substrate (100 nM primer-template) as indicated. ^{32}P-Labeled 24-mer primer was extended in the presence of all four dNTPs. The reaction products were analyzed by denaturing gel electrophoresis with subsequent phosphorimaging analysis.

EDTA in 95% formamide (v/v). Products were analyzed by electrophoresis, as described for the steady-state experiments.

RESULTS

Primer Extension by Human REV1 in the Presence of All Four dNTPs—Polymerization by human REV1 at various N^2- and O^6-modified G adducts was analyzed in "standing start" assays using 24-mer/36-mer duplexes containing G and each of 11 different N^2-G and O^6-G adducts (Fig. 1) at position 25 of the template (Fig. 2). Increasing concentrations of REV1 were used in 15-min incubations with each of 12 different primer-template complexes in the presence of all four dNTPs. REV1 readily incorporated one base on the 3′-end of the 24-mer primer annealed to unmodified G and all of the N^2-modified G templates, in proportion to enzyme concentration, but extended poorly across subsequent nonguanine (C and T) positions 26 and 27 of templates except for the cases of the G and N^2-MeG templates. Opposite N^2-AnthG and N^2-BPG, REV1 did incorporate one base but with a gradual reduction in extension products. Polymerization across O^6-MeG and O^6-BzG yielded a pattern of extension similar to N^2-G adducts, but each of the extension products was less than the insertion product formed across N^2-MeG and N^2-BzG, respectively. In contrast, all polymerization by REV1 was almost completely blocked opposite O^6-PobG.

Steady-state Kinetics of dNTP Incorporation Opposite G and N^2-G and O^6-G Adducts—Steady-state parameters were measured for dNTP incorporation into 24-mer/36-mer duplexes opposite G, N^2-G, and O^6-G adducts by REV1 (Tables 2 and 3). The incorporations of dATP opposite G, N^2-G, and O^6-G adducts were not determined because of much less efficient activity than with other dNTPs. REV1 preferentially incorporated dCTP opposite G and all of the modified G adducts, with relatively low misinsertion frequency for dTTP and dGTP ($f = 0.006–0.06$), where $f = (k_{cat}/K_m)_{dNTP}/(k_{cat}/K_m)_{dCTP}$ (with dNTP $\neq$ dCTP). Most N^2- and O^6-modifications at G increased the misinsertion frequencies of dGTP and dTTP 1.1–9-fold. The increase in the misinsertion frequencies of dGTP and dTTP was highest (4- and 9-fold) with

mass equation $[E_f] = [E_t] - [E{\cdot}DNA]$, in which $[E_t]$ = total enzyme concentration in reaction mixture and $[E{\cdot}DNA]$ = the concentration of enzyme-DNA complex.

REV1-catalyzed Pyrophosphorolysis—REV1 (50 nM) was preincubated with 100 nM ^{32}P-labeled 25-mer/36-mer primer-template DNA in a reaction mixture containing 50 mM Tris-HCl (pH 7.5), 50 mM NaCl, 50 mM MgCl$_2$, 5 mM dithiothreitol, 100 μg ml^{-1} bovine serum albumin (w/v), and 10% glycerol (v/v) on ice for 15 min. Pyrophosphorolysis was then initiated by the addition of various concentrations of PP$_i$ to a preincubated *E·DNA* mixture. After 15 min at 37 °C, the reactions were quenched with 10 volumes of a solution of 20 mM

TABLE 2

Steady-state kinetic parameters for one-base incorporation opposite guanine N^2 adducts by human REV1

Template	dNTP	K_m	k_{cat}	k_{cat}/K_m	f(misinsertion ratio)
		μM	s^{-1}	$mM^{-1} s^{-1}$	
G	C	13 ± 2	0.0120 ± 0.0004	0.92	1
	G	250 ± 50	0.0014 ± 0.0001	0.0056	0.0061
	T	350 ± 60	0.0021 ± 0.0001	0.0060	0.0065
N^2-MeG	C	25 ± 2	0.0088 ± 0.0002	0.35	1
	G	170 ± 40	0.00064 ± 0.00004	0.0038	0.011
	T	440 ± 90	0.0015 ± 0.0001	0.0034	0.010
N^2-EtG	C	9.4 ± 1.8	0.0046 ± 0.0002	0.49	1
	G	290 ± 90	0.0014 ± 0.0001	0.0048	0.010
	T	400 ± 60	0.0019 ± 0.0001	0.0048	0.010
N^2-IbG	C	22 ± 3	0.0124 ± 0.0004	0.56	1
	G	260 ± 80	0.0034 ± 0.0004	0.013	0.023
	T	380 ± 50	0.0049 ± 0.0002	0.013	0.023
N^2-BzG	C	6.9 ± 0.6	0.0085 ± 0.0002	1.2	1
	G	180 ± 40	0.0040 ± 0.0003	0.022	0.018
	T	310 ± 70	0.0051 ± 0.0004	0.016	0.013
N^2-NaphG	C	4.4 ± 0.2	0.0041 ± 0.0001	0.93	1
	G	220 ± 60	0.0025 ± 0.0002	0.011	0.012
	T	230 ± 30	0.0015 ± 0.0001	0.0065	0.0070
N^2-AnthG	C	7.8 ± 1.5	0.0024 ± 0.0001	0.31	1
	G	100 ± 20	0.0014 ± 0.0001	0.014	0.045
	T	320 ± 60	0.0023 ± 0.0002	0.0072	0.023
N^2-BPG	C	2.3 ± 0.3	0.002 ± 0.0001	0.87	1
	G	70 ± 10	0.00084 ± 0.00003	0.012	0.014
	T	80 ± 10	0.0011 ± 0.0001	0.014	0.016

TABLE 3

Steady-state kinetic parameters for one-base incorporation opposite guanine O^6 adducts by human REV1

Template	dNTP	K_m	k_{cat}	k_{cat}/K_m	f(misinsertion ratio)
		μM	s^{-1}	$mM^{-1} s^{-1}$	
G	C	13 ± 2	0.012 ± 0.001	0.92	1
	G	250 ± 50	0.0014 ± 0.0001	0.0056	0.0061
	T	350 ± 60	0.0021 ± 0.0001	0.0060	0.0065
O^6-MeG	C	60 ± 10	0.0034 ± 0.0001	0.057	1
	G	190 ± 20	0.000071 ± 0.000001	0.00037	0.0065
	T	360 ± 40	0.00043 ± 0.00002	0.0012	0.021
O^6-BzG	C	40 ± 10	0.0083 ± 0.0002	0.21	1
	G	250 ± 60	0.0030 ± 0.0002	0.012	0.057
	T	330 ± 50	0.0012 ± 0.0001	0.0036	0.017
O^6-PobG	C	120 ± 30	0.000018 ± 0.000001	0.00015	1

FIGURE 3. **Pre-steady-state burst kinetics of incorporation opposite G, N^2-BzG, N^2-NaphG, N^2-AnthG, N^2-BPG, O^6-MeG, O^6-BzG, and O^6-PobG by human REV1.** REV1 (120 nM) was incubated with 100 nM 24-mer/36-mer primer-template complex in the rapid quenched-flow instrument and mixed with 1 mM dCTP (and MgCl$_2$) to initiate reactions. *A*, G and N^2-G adducts: 24-mer/36-G-mer (■), 24-mer/36-N^2-BzG-mer (▲), 24-mer/36-N^2-NaphG-mer (▼), 24-mer/36-N^2-AnthG-mer (♦), 24-mer/36-N^2-BPG-mer (●). *B*, G and O^6-G adducts: 24-mer/36-G-mer (■), 24-mer/36-O^6-MeG-mer (▲), 24-mer/36-O^6-BzG-mer (▼), and 24-mer/36-O^6-PobG-mer (♦). All polymerization reactions were quenched with 0.3 M EDTA at various time intervals. The data were fit to the burst equation $y = A(1 - e^{-kpt}) + k_{ss}t$, as described under "Experimental Procedures" (without normalization of k_{ss} for enzyme concentration in the equation). The following rates were estimated: G-mer, $k_p = 0.43 \pm 0.13\ s^{-1}$, $k_{ss} = 0.015 \pm 0.001\ s^{-1}$; N^2-BzG-mer, $k_p = 0.62 \pm 0.21\ s^{-1}$, $k_{ss} = 0.014 \pm 0.001\ s^{-1}$; N^2-NaphG-mer, $k_p = 0.22 \pm 0.07\ s^{-1}$, $k_{ss} = 0.0045 \pm 0.0008\ s^{-1}$; N^2-AnthG-mer, $k_p = 0.26 \pm 0.09\ s^{-1}$, $k_{ss} = 0.0033 \pm 0.0008\ s^{-1}$; N^2-BPG-mer, $k_p = 0.88 \pm 0.22\ s^{-1}$, $k_{ss} = 0.0028 \pm 0.0006\ s^{-1}$; O^6-MeG-mer, $k_p = 0.08 \pm 0.03\ s^{-1}$, $k_{ss} = 0.0037 \pm 0.0007\ s^{-1}$; O^6-BzG-mer, $k_p = 0.15 \pm 0.05\ s^{-1}$, $k_{ss} = 0.0056 \pm 0.0004\ s^{-1}$.

tions, REV1 showed much lower catalytic efficiencies (13- and 5-fold, respectively) opposite O^6-MeG than opposite unmodified G and no detectable activity opposite O^6-PobG.

Pre-steady-state Kinetics of dCTP Incorporation Opposite G, N^2-BzG, N^2-BPG, O^6-BzG, and O^6-PobG by REV1—In order to characterize the kinetics within the polymerization cycle of REV1, pre-steady-state reactions were performed in a rapid quench flow instrument. Preformed E·DNA complexes were mixed with saturating concentrations of dCTP-Mg^{2+} and then quenched following varying reaction times (Fig. 3). Interestingly, REV1 showed an apparent burst for the correct dCTP incorporation opposite N^2-BPG but just a marginally noticeable burst opposite G, N^2-BzG, or O^6-BzG. These results indicate that steps after product formation are at least partially rate-limiting in catalysis with N^2-BPG but not with G, N^2-BzG, and O^6-BzG. The first phase of the cycle (*i.e.* the burst phase) was finished in ~1 s with the N^2-BPG template. REV1 incorporation of dCTP into the 24-mer/36-N^2-BPG-mer occurred with a burst rate of $k_p = 0.88 \pm 0.22\ s^{-1}$ and 5% burst amplitude (the percentage of REV1-forming product in the burst phase), which might represent the active fraction of REV1 in a catalytically adequate conformation with N^2-BPG, dCTP, and amino acid residues in the active site under these experimental conditions or the presence of other nonproductive DNA binding complexes with duplex DNA. The dCTP incorporation opposite G, N^2-BzG, and O^6-BzG showed lower pre-steady-state rates than opposite N^2-BPG (if indeed this is even a valid "burst"). The pre-steady-state rate opposite N^2-BzG was 2-fold higher than O^6-BzG, indicating that product formation opposite the N^2-G adduct is more efficient than O^6-BzG. However, the k_{ss} rate in the second phase (steady-state) was much lower with N^2-BPG than with G, N^2-BzG, and O^6-BzG, in good agreement with the k_{cat} values. The k_{ss} rate (0.015 s^{-1}) opposite unmodified G was similar to the k_{cat} value (0.012 s^{-1}) obtained from the independ-

O^6-BzG and N^2-AnthG, respectively, and was attributable to the decreased k_{cat}/K_m value for the correct dCTP insertion and the increased k_{cat}/K_m values of dGTP and dTTP insertion.

For the correct incorporation of dCTP, REV1 showed catalytic efficiencies (k_{cat}/K_m) opposite N^2-modified G adducts similar to unmodified G, whereas REV1 showed severely reduced catalytic efficiencies opposite O^6-G adducts (*e.g.* 16-fold with O^6-MeG and 6000-fold with O^6-PobG). Notably, the value of k_{cat}/K_m with the N^2-BPG template was nearly the same as that with the G template, although the values of K_m and k_{cat} with N^2-BPG were both 6-fold lower than that with G. REV1 showed 6-fold greater catalytic efficiencies with N^2-MeG and N^2-BzG than those with O^6-MeG and O^6-BzG, respectively, indicating that the N^2-G adduct is preferable to the O^6-G adduct as a template base for polymerization by REV1. The large decrease (6000-fold) of k_{cat}/K_m for dCTP incorporation opposite O^6-PobG was due to both the decrease of k_{cat} and the increase of K_m. Interestingly, REV1 also showed 4-fold greater catalytic efficiencies with the benzyl adducts at guanine N2 or O6 than the methyl adducts at the corresponding position, indicating that a larger but aromatic benzyl group adducted to guanine offers some advantage for REV1 polymerization over a smaller methyl group. For the incorrect dGTP and dTTP incorpora-
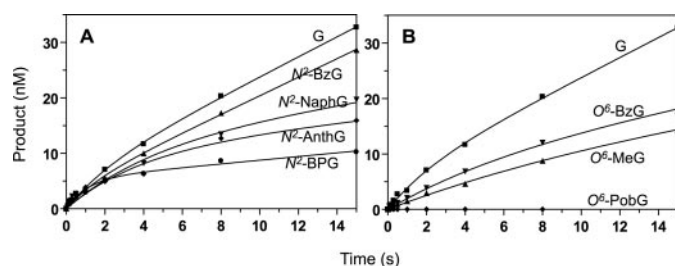
ent steady-state kinetic analysis. For the oligonucleotides containing O^6-PobG, dCTP incorporation was undetectable.

Phosphorothioate Analysis of dC—In considering whether the chemistry step (phosphodiester bond formation) by REV1 might be rate-limiting during the polymerization cycle, we compared the rates of incorporation of dCTP and (S_p)-dCTPαS opposite N^2-BPG. The pre-steady-state burst rates of incorporation opposite N^2-BPG were determined in a rapid quench instrument using dCTP and (S_p)-dCTPαS. Similar to a kinetic isotope effect, the sulfur substitution of α-oxygen at dCTP makes bond breakage more difficult. If the chemistry step is slow and rate-limiting in a reaction, the overall reaction should be slowed by dCTPαS compared with dCTP (42). Incorporation of (S_p)-dCTPαS opposite N^2-BPG yielded no significant difference in the burst rate compared with dCTP (Fig. 4), indicating that the chemistry step may not be rate-limiting in the polymerization cycle opposite N^2-BPG.
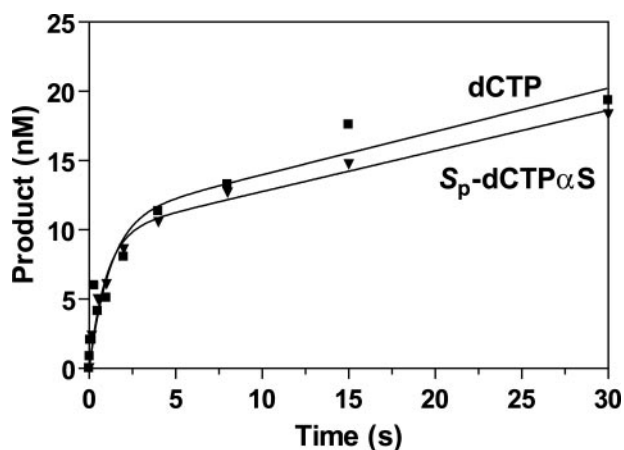

FIGURE 4. **Phosphorothioate analysis of pre-steady-state kinetics of dCTP incorporation opposite N^2-BPG by human REV1.** REV1 (240 nM) was incubated with 100 nM 24-mer/36-mer primer-template complex in the rapid quenched-flow instrument and mixed with 1 mM dCTP (■) or (S_p)-dCTPαS (▼) to initiate reactions for the 24-mer/36-N^2-BPG-mer. The pre-steady-state rates were determined from the burst equation and are indicated in the figure. The following rates were estimated: dCTP, $k_p = 0.83 \pm 0.29$ s^{-1}; (S_p)-dCTPαS, $k_p = 1.0 \pm 0.2$ s^{-1}.

Determination of K_d^{dCTP} for dCTP Incorporation by REV1—Analysis of the change of the pre-steady-state rate as a function of increasing dNTP concentration yields K_d^{dNTP}, a measure of the binding affinity of the dNTP to the E·DNA binary complex to form a ternary complex poised for catalysis (39, 40). The observed pre-steady-state rates (k_{obs}) were plotted as a function of dNTP and fit to a hyperbolic equation, yielding a k_{pol} (maximal rate of nucleotide incorporation) of 0.87 ± 0.02 s^{-1} and a K_d^{dCTP} of 40 ± 4 μM with the unmodified DNA substrate and a k_{pol} of 0.90 ± 0.02 s^{-1} and a K_d^{dCTP} of 99 ± 9 μM with the N^2-BPG-containing DNA substrate (Fig. 5), indicating that the presence of N^2-BPG in the template may make REV1 bind dCTP less tightly (~2.5-fold) than unmodified G. The K_d^{dCTP} value of REV1 is about 4-fold lower than for other Y family DNA polymerases ($K_d^{dCTP} \cong 140-360$ μM) (20–22) but much higher than replicative DNA polymerases (K_d^{dCTP}, 1–4 μM) (*e.g.* pol T7$^-$ and human immunodeficiency virus type 1 reverse transcriptase) (18, 43), indicating that REV1 has a slightly higher binding affinity for dCTP opposite G than other Y family polymerases but much lower binding affinity than replicative polymerases.

Binding of REV1 to DNA Containing G and N^2-BPG—An apparent dissociation constant (K_d^{DNA}) of REV1 for primer-template DNA substrate was estimated using an electrophoretic mobility shift assay. Electrophoretic mobility shift assays can provide some quantitative data for protein-nucleic acid binding, although it does not represent a true equilibrium constant (44). The fraction of primer-template DNA shifted by REV1 was determined and used as an indicator for DNA binding of REV1. The data clearly indicate enhanced binding of the N^2-BPG-DNA, as seen in the 40 and 80 nM REV1 lanes (Fig. 6, *A* and *B*). The K_d value of REV1 for unmodified DNA (24-mer/36-G-mer) was 180 ± 8 nM, which was about 3-fold higher than that for N^2-BPG-adducted DNA (24-mer/36-N^2-BPG-mer) (Fig. 6C), indicating that the binding affinity of DNA to REV1 is significantly increased by the presence of N^2-BPG adduct.

Pyrophosphorolysis on 25-Mer/36-Mer—The pyrophosphorolysis activity of REV1 (*i.e.* reversal of the polymerization reaction) was measured with 25-C-mer/36-G (or N^2-G-adduct)-mer primer-template complexes in the presence of PP$_i$. Dpo4, a Y family DNA polymerase from *Sulfolobus solfataricus*, has robust pyrophosphorolysis activity, which may possibly affect its fidelity, but human pol η, ι, and κ do not (45). Human REV1 (50 nM) showed only trace degradation (1–2%) of 25-mer primer even in the presence of 0.5–2 mM PP$_i$, which was similarly observed with G and bulky N^2-G-adduct-containing DNA (Fig. S2). These results indicate that REV1 has only minimal pyrophosphorolysis activity, which appears not to be changed by the presence of a bulky N^2-G adduct.
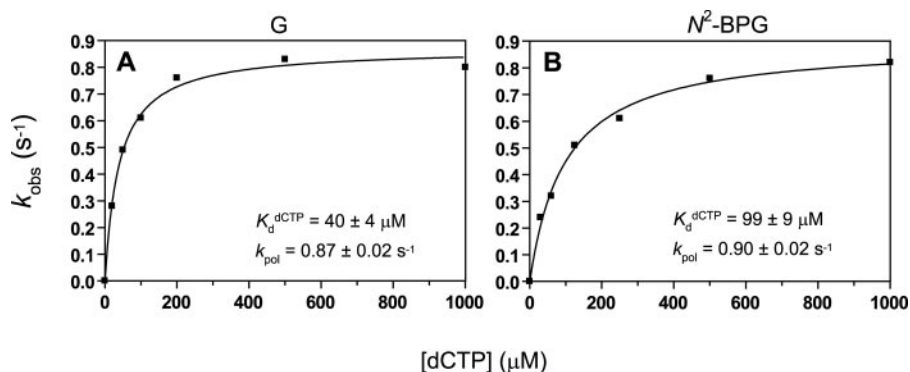

FIGURE 5. **Determination of k_{pol} and K_d^{dCTP} with human REV1 for incorporation of dCTP opposite G and N^2-BPG.** *A*, a 10-fold excess of REV1 (300 nM) was incubated with 30 nM 24-mer/36-G-mer primer-template complex in the rapid quenched-flow instrument and mixed with increasing dCTP concentrations (■, 20–1000 μM) to initiate the single turnover reactions. *B*, REV1 (240 nM) was incubated with 100 nM 24-mer/36-N^2-BPG-mer primer-template complex in the rapid quenched-flow instrument and mixed with increasing dCTP concentrations (■, 30–1000 μM) to initiate the reaction. Reactions were quenched with EDTA. A plot of observed rates of nucleotide incorporation (k_{obs}) *versus* [dCTP] was fit to a hyperbolic equation, as described under "Experimental Procedures." *A*, G (unmodified): k_{pol} (maximal rate of nucleotide incorporation) = 0.87 ± 0.02 s^{-1} and K_d^{dCTP} = 40 ± 4 μM; *B*, N^2-BPG: k_{pol} = 0.90 ± 0.02 s^{-1} and K_d^{dCTP} = 99 ± 9 μM.

Comparison of Primer Extension in the Presence of All Four dNTPs and Steady-state Kinetic Parameters of One-base Incorporation Opposite N^2-EtG and N^2,N^2-diMeG by Human REV1— In order to examine the role of an N2 hydrogen atom of N^2-G adducts during polymerization by REV1, bypass abilities were compared opposite N^2-EtG and N^2,N^2-diMeG using primer extension and steady-state kinetic analysis. Polymerization of human REV1 opposite N^2-EtG and N^2,N^2-diMeG was analyzed in "standing start" assays using 24-mer/36-mer duplexes containing N^2-EtG and N^2,N^2-diMeG (Fig. 1) at position 25 of the template (Fig. 2A). Increasing concentrations of REV1 were used in 15-min incubations with each of both primer-template complexes in the presence of all four dNTPs. REV1 showed similar one-base exten-

FIGURE 6. **Estimation of the apparent K_d^{DNA} for REV1 to 24-mer/36-G-mer and 24-mer/36-N^2-BPG-mer by electrophoretic mobility shift assay.** A, 24-mer/36-G-mer; B, 24-mer/36-N^2-BPG-mer. Reaction mixtures containing 0.5 nm of ³²P-labeled 24-mer/36-mer primer-template duplex DNA were incubated with increasing concentrations of human REV1 (2.5–320 nm) and resolved on a 4% nondenaturing polyacrylamide gel to separate the free DNA and the REV1-DNA complexes. C, the fractions of REV1-bound DNA were plotted against the concentrations of free human REV1. Data were fit to a single-site binding equation, as described under "Experimental Procedures." The fitted values of the apparent K_d^{DNA} are indicated in the figure. The following values of K_d were estimated: 24-mer/36-G-mer (■), 180 ± 10 nm; 24-mer/36-N^2-BPG-mer (▲), 59 ± 5 nm.

sion ability opposite N^2-EtG and N^2,N^2-diMeG. This result was consistent with the steady-state kinetic analysis of one-base incorporation (Table 4). REV1 showed no decrease but rather a slight increase (1.6-fold) of k_{cat}/K_m in dCTP incorporation opposite N^2,N^2-diMeG compared with N^2-EtG. Interestingly, REV1 demonstrated much higher misincorporation of dGTP and dTTP (5- and 8-fold, respectively) opposite N^2,N^2-diMeG compared with N^2-EtG, indicating that the shape of the chemical moiety at guanine N2 can also affect the preference of dNTP opposite N^2-G adducts by REV1.

DISCUSSION

In this study, we provide kinetic evidence that REV1 is considerably more competent for dCTP incorporation opposite large N^2-modified G lesions compared with O^6-modified G lesions. We investigated the effect of adducts at guanine N2 and O6 atoms of a DNA substrate on the polymerization ability and the fidelity by REV1 using steady-state and pre-steady-state kinetic analyses. Although having the lowest maximal polymerization rate (k_{pol} 0.9 s^{-1}) opposite unmodified G among human Y family DNA polymerases, REV1 achieved the correct dCTP incorporation opposite all N^2-G lesions (including the largest N^2-BPG) with catalytic efficiency similar to that opposite the unmodified G. In contrast, the lesions at the G O6 atom noticeably attenuated the ability of dCTP incorporation opposite lesion by REV1, ultimately leading to the almost complete loss of the ability opposite O^6-PobG. The presence of an apparent burst only with N^2-BPG but little with G suggests that the late steps *after* product formation may be considerably slowed by a relatively large lesion (*e.g.* BP) at guanine N2 during catalysis (*e.g.* release of the oligonucleotide). No significant decrease of catalytic efficiency in polymerization opposite N^2,N^2-diMeG was observed compared with N^2-EtG (Table 4), suggesting that REV1 does not require a hydrogen atom at guanine N2 for efficient polymerization, consistent with the use of the hydrogen bonding with a protein-template (Arg) instead of a guanine template (34).

Comparisons of abilities and fidelities of REV1 to polymerize opposite N^2- and O^6-G adducts provide detailed information about catalytic behavior of REV1 opposite those guanine lesions. We performed the kinetic comparison according to the variable of adduct size at both guanine N2 and O6, as done previously with other DNA polymerases (17, 20–23). Our approach using two series of N^2- and O^6-G adducts has an inherent limitation in that the chemical substitution at the N2 or O6 atom can change not only the size but also the other chemical properties, such as hydrophobic and electronic factors. For example, the hydrophobicity of guanine adducts grad-
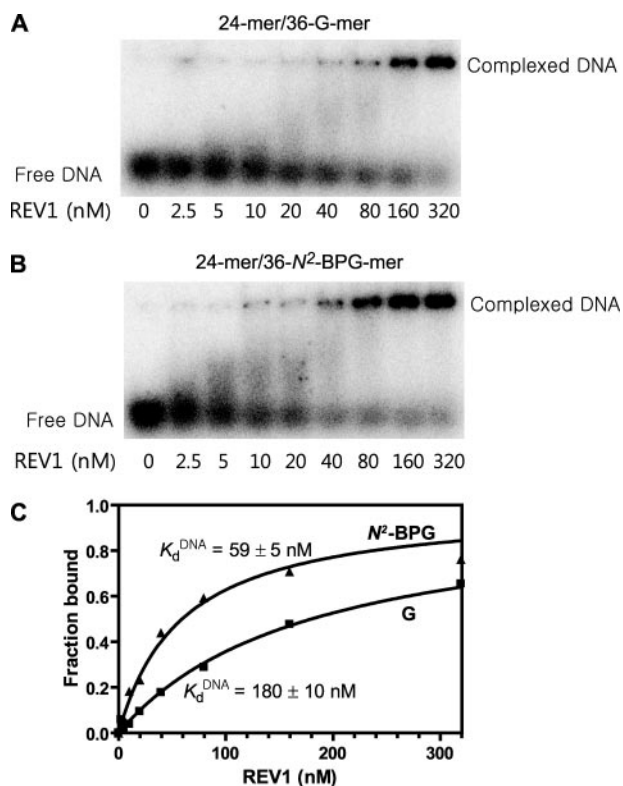
TABLE 4
Comparison of steady-state kinetic parameters for one-base incorporation opposite N^2-EtG and N^2,N^2-diMeG by human REV1

| Template: dNTP	K_m	k_{cat}	k_{cat}/K_m	-Fold difference of k_{cat}/K_m compared with N^2-EtG	f (misinsertion ratio)
	μM	s^{-1}	$mM^{-1} s^{-1}$	-fold	
N^2-EtG: dCTP	9.4 ± 1.8	0.0046 ± 0.0002	0.49		1
N^2,N^2-diMeG: dCTP	10 ± 2	0.0080 ± 0.0003	0.80	1.6-fold higher	1
N^2-EtG: dGTP	290 ± 90	0.0014 ± 0.0001	0.0048		0.010
N^2,N^2-diMeG: dGTP	190 ± 50	0.0030 ± 0.0002	0.016	3-fold higher	0.046
N^2-EtG: dTTP	400 ± 60	0.0019 ± 0.0001	0.0048		0.010
N^2,N^2-diMeG: dTTP	140 ± 40	0.0039 ± 0.0003	0.028	6-fold higher	0.080
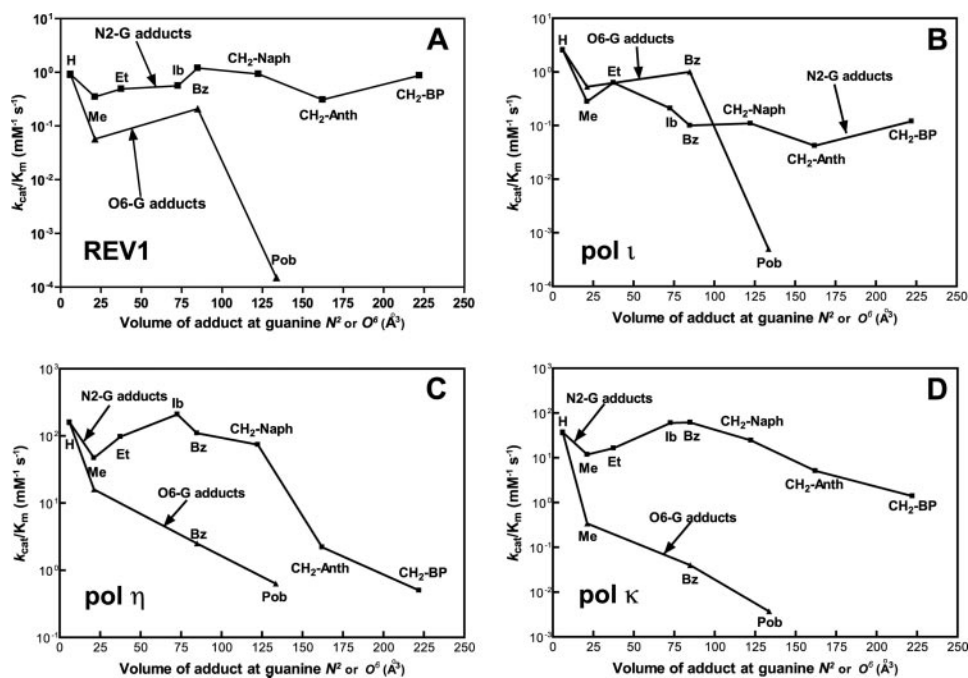
FIGURE 7. **Relationship of the volume of adduct at the guanine N2 and O6 atoms with catalytic efficiency (k_{cat}/K_m) for dCTP incorporation opposite N^2-G and O^6-G adducts by human Y family polymerases.** The molecular volumes (Å³) of adducts at the guanine N2 or O6 atom were calculated using the program Chem3D (version 7.0) based on the Connolly surface algorithm (56) and plotted against k_{cat}/K_m values (Table 2) for dCTP incorporation for various N^2-G adducts (■) and O^6-G adducts (▲) by four Y family DNA polymerases. The k_{cat}/K_m values for pol η, pol ι, and pol κ were adapted from previous reports from this laboratory (20–23). *A*, REV1; *B*, pol ι; *C*, pol η; *D*, pol κ.

ually increases along with the steric bulk (alkyl and alkaryl group) in these series, but we cannot separate these effects (21). Nonetheless, the information is still useful in understanding how different DNA polymerases handle various DNA modifications during DNA synthesis (17, 20–23). A plot of the catalytic specificity constants (k_{cat}/K_m) *versus* the molecular volume of the substituent at the guanine N2 or O6 atom (Fig. 7*A*) indicates that REV1 is remarkably tolerant of relatively large lesions at guanine N2 compared with guanine O6. Although this catalytic feature has some similarity with other Y family DNA polymerases, REV1 is apparently the most resilient in catalysis against the larger adducts at guanine N2 among these four Y family DNA polymerases (Fig. 7, *A–D*). We found that the k_{cat}/K_m values for dCTP incorporation opposite various N^2-G adducts by REV1 are very similar to that opposite unmodified G in steady-state kinetics (Table 2). Even the largest, N^2-BPG, did not significantly decrease k_{cat}/K_m for dCTP incorporation. This pattern is compatible with pre-steady-state kinetic results (Fig. 3) in that REV1 incorporated dCTP opposite N^2-BPG at the maximal rate of polymerization (k_{pol}) nearly the same as opposite unmodified G, despite the slight decrease in binding affinity of dCTP (Fig. 5). Thus, none of the factors of N2 substitution at guanine appears to hinder the catalysis of REV1 much. In contrast, the bulky modifications at template guanine O6 severely decreased the k_{cat}/K_m for dCTP incorporation by REV1 (up to 6,000-fold), compared with the unmodified G (Table 3). Thus, the large Pob group at guanine O6 almost abolished the catalytic activity of REV1 in the standing start primer extension (Fig. 2*B*). We cannot discern if O^6-PobG-induced blockage is largely due to the steric or other factors

(*e.g.* increased hydrogen-bonding capability and hydrophobicity) of O^6-PobG. However, it is clear that a bulky O^6-G adduct, O^6-PobG, almost completely blocks REV1, in contrast with pol η (23). REV1 retained relatively high fidelity ($f = 0.006 – 0.06$) in nucleotide incorporation opposite various N^2- and O^6-G adducts (Table 2 and 3), consistent with a catalytic role mainly as a dCTP transferase. However, although the initial recognition of dCTP is by an arginine, REV1 catalysis can be slowed by a large lesion.

The pre-steady-state kinetic analysis indicated a lack of burst kinetics in the incorporation of dCTP opposite G (Fig. 3*A*). With the O^6-substituted G adducts (Fig. 3*B*), substitution slowed the rate but had no effect on the shape of the time course. However, increasing bulk (or, alternatively, hydrophobicity or aromaticity) at the N2 atom produced a trend with an increasing burst pattern (Fig. 3*A*). The apparent burst (finished in ~1 s) amplitude only accounted for ~5% of that corresponding to one molecule of product formed by one REV1 protein (REV1 quantified by UV) in the case of REV1. The k_{pol} was estimated to be ~1 s⁻¹, consistent with single-turnover studies in which a similar k_{pol} was estimated for dCTP insertion opposite G or N^2-BPG (Fig. 5). The kinetics of dCTP insertion opposite N^2-BPG were not affected by the sulfur-substituted (S_p)-dCTPαS (Fig. 4). These results are consistent with a step following product formation being rate-limiting only in the case of the bulky N^2-substituted G template. This step could be product release, in that electrophoretic mobility shift experiments indicated 3-fold tighter binding of REV1 to the N^2-BPG-containing DNA than the unmodified DNA (Fig. 6), and this result may be congruent with a 5-fold decrease in k_{ss} (Fig. 3*A*). The lack of change in the ratio k_{cat}/K_m with increasing bulk or hydrophobicity at the N2 atom would be consistent with the decreasing k_{cat} (possibly decreasing k_{off} for the product) and a decreasing K_m (possibly decreasing K_d), although the exact interpretation of K_m is not straightforward in these systems (46).

An unexplained issue is why only partial bursts were seen with the N^2-BPG-adducted oligonucleotide (Figs. 3*A* and 4). One possible explanation is that the purified REV1 preparation is only partially active. An alternative explanation is one advanced for the action of some replicative DNA polymerases at some DNA adducts, namely that the burst represents the fraction of the ternary DNA-polymerase·dCTP complex existing in a conformationally active form for rapid insertion (Fig. 8) (47, 48). Kinetic modeling can readily be done to obtain such fits to the data (47), although in this case there are not enough independent boundaries to make the exercise very definitive.
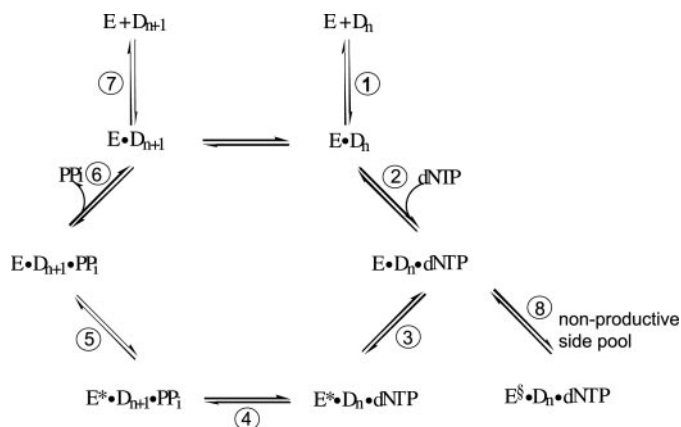
FIGURE 8. **General kinetic mechanism for DNA polymerization.** Individual steps are numbered. E, polymerase; D_n = DNA substrate; E^*, conformationally altered polymerase; $E^\S$, nonproductive conformation of polymerase; D_{n+1} = DNA extended by 1 base.

The lesions at guanine N2 in the DNA substrate only slightly affected the affinity for the correct dCTP of REV1. We found only a 2.5-fold change in the K_d^{dCTP} for insertion opposite G and N^2-BPG in a detailed kinetic analysis under apparent single-turnover conditions (Fig. 5). This small effect was also similarly observed in the previous report of pol κ with N^2-AnthG (20). The finding that only a small decrease was observed in the K_d^{dCTP} for insertion opposite a bulky N^2-G adduct contrasts with the results of Howell *et al.* (49) with yeast Rev1, who reported a very low K_d^{dCTP} for incorporation opposite G (0.78 μM) and much higher K_d^{dCTP} values for incorporation opposite an abasic site (28 μM) and 7,8-dihydro-8-oxoG (210 μM) (*cf.* 40 and 99 μM for G and N^2-BPG in our study; Fig. 5). However, the yeast Rev1 enzyme used by Howell *et al.* (49) has a C-terminal truncation of 239 residues and may not be comparable with the full-length human REV1 enzyme we used.

Which steps of the catalytic cycle in the kinetic scheme of REV1 (Fig. 8) can be affected by the lesions at guanine N2? The same maximal polymerization rates opposite G and N^2-BPG, the slight decrease of K_d^{dCTP} by N^2-BPG, and no significant elemental effect with (S_p)-dCTPαS on polymerization for N^2-BPG suggest that the steps for product formation (*e.g.* the formation of phosphodiester bond) (Fig. 8, *step 4*), the conformational change (*step 3*), and dNTP binding (*step 2*) were not largely interfered with by N^2-BPG. The contribution of reverse polymerization by REV1 also appears to be almost negligible from C:G and C:N^2-G adducts in that pyrophosphorolysis was only minimal even at high concentrations of PP$_i$ (Fig. S2). Although the elemental effects by dNTPαS are not without controversy regarding interpretation due to the varied transition states among different polymerases (42), the existence of major differences in these values among polymerases and specific DNA adducts argues that they should be considered carefully. Interesting results were obtained in the experiments of pre-steady-state burst kinetics for dCTP incorporation opposite G and N^2-G adducts. No apparent burst with unmodified G suggests that steps preceding the chemistry step (*e.g.* the conformational change) might be rate-limiting for polymerization opposite unmodified G. However, the appearance of a burst with the N^2-BPG and the higher binding affinity of REV1 to N^2-BPG-containing DNA suggest that the late steps after the chemistry step, possibly product release (*step 7*), might be largely affected by N^2-BPG and thus become at least partially rate-limiting in the overall catalysis. One possibility is that slowed REV1 release after the product formation opposite N^2-BPG might provide a time interval sufficient for switching of REV1 to the other extender polymerases (*e.g.* pol κ and ζ) efficient for the subsequent extension in TLS events. We note a very recent report on pre-steady-state kinetics by yeast Rev1 protein, concluding that the nucleotide binding step can be interfered with during dCTP incorporation opposite nonguanine templates (49). However, the k_{pol} estimated in that work was only 0.012 s^{-1}, and the experiments do not appear to involve true pre-steady-state conditions.

The data collection for recombinant human pols η, ι, κ, and REV1 now allows several comparisons among human Y family DNA polymerases (20–23). The major difference between Y family polymerases is in the rates of polymerization (*i.e.* k_{pol}). The k_{pol} (or at least k_p) with REV1 (0.9 s^{-1}) is much less than for pols η, ι, and κ (40, 4, and 13 s^{-1}, respectively) for dCTP incorporation opposite unmodified G. But for the large N^2-G adducts, the k_{pol} with REV1 (0.9 s^{-1} with N^2-BPG) is relatively higher than for pol η (0.24 s^{-1} with N^2-BPG) and pol ι (0.16 s^{-1} with N^2-AnthG) although less than pol κ (5.9 s^{-1} with N^2-BPG), indicating that REV1 has a relatively proficient catalytic ability for the accurate synthesis opposite large N^2-G adducts, similar to pol κ. However, REV1 has no ability as a proficient extender past the lesion, unlike pol κ, and thus REV1 could be replaced by other extender polymerases for the rest of the lesion bypass process. In the analyses of the effects of guanine adducts on k_{cat}/K_m for dCTP incorporation with Y family pols, the effect of substitution at the O6 atom, especially with O^6-PobG, is generally much more severe than that seen at N2 (Fig. 7). With pol ι and REV1, however, no or only a low effect is found for relatively small O^6-adducts, such as O^6-MeG or O^6-BzG, compared with pols η and κ (Fig. 7, *A* and *B*). These results can be partially explained by base-pairing modes and the structures in the active site of each polymerase. For pols η and κ, which require Watson-Crick base pairing for efficient catalysis (50, 51), dCTP is more efficiently incorporated opposite N^2-G adducts than O^6-G adducts, because optimal Watson-Crick hydrogen bonding is possible only with N^2-G adducts but not with O^6-G adducts. This view would be consistent with recent reports that the *S. solfataricus* Y family DNA polymerase Dpo4 forms a wobble base pair between C and O^6-MeG (or O^6-BzG), and thus the polymerization is inhibited (52, 53). Nevertheless, pol η, apparently the most efficient Y family polymerase for bypass opposite O^6-PobG, might have an active site spacious enough to accommodate a large O^6-PobG. For pol ι, known to require Hoogsteen base pairing for efficient catalysis (54), the relatively large lesion O^6-PobG (but not O^6-MeG and O^6-BzG) might induce steric hindrance near the O^6 position of G in the active site and thus interfere in the formation of Hoogsteen base pairing with an incoming dCTP. In contrast, REV1

may uniquely utilize an Arg for the optimal hydrogen bonding with an incoming dCTP, as shown with yeast Rev1 (34). The Hoogsteen edge of template G forms hydrogen bonds with the G loop residues of REV1, and thus the relatively large lesion O^6-PobG (but not O^6-MeG or O^6-BzG), might sterically clash with the G-loop of REV1 to interfere with catalysis (compared with N^2-adducts, which are sterically unhindered) (34). However we cannot exclude the possibility that other chemical properties, such as increased hydrogen bonding capability of a Pob group (via pyridyl ring and carbonyl oxygen) or aromaticity of a B[a]P group, interfere with or facilitate the catalysis opposite guanine lesions by interactions with REV1 and DNA. Dispensability of the Watson-Crick hydrogen bonding between template G and dCTP might enable REV1 to retain an intrinsic ability for efficient and accurate bypass opposite specific guanine lesions that can mask the Watson-Crick face but not Hoogsteen edge (*e.g.* ring-closed 1,N^2-etheno-G, malondialdehyde-G, and bulky C^8-G adducts). Thus, detailed kinetic analyses for testing this hypothesis are possible. Consistent with this view, a very recent crystallographic report demonstrates that yeast Rev1 accommodates the exocyclic 1,N^2-propano-dG adduct well in the active site (55).

In conclusion, our results suggest that, among Y family DNA polymerases, human REV1 is very tolerant of bulky lesions at guanine N2 (least up to N^2-BPG) for catalysis but poorly at guanine O6. The unique ability of REV1 for highly selective dCTP incorporation opposite various N^2- and O^6-guanine adducts also suggests that REV1 may play a catalytic role in an error-free bypass opposite certain types of guanine DNA lesions.

REFERENCES

1. Friedberg, E. C., Walker, G. C., Siede, W., Wood, R. D., Schultz, R. A., and Ellenberger, T. (2006) *DNA Repair And Mutagenesis*, 2nd Ed., American Society for Microbiology Press, Washington, DC
2. Guengerich, F. P. (2006) *Chem. Rev.* **106,** 420–452
3. Goodman, M. F. (2002) *Annu. Rev. Biochem.* **71,** 17–50
4. Prakash, S., Johnson, R. E., and Prakash, L. (2005) *Annu. Rev. Biochem.* **74,** 317–353
5. Ohmori, H., Friedberg, E. C., Fuchs, R. P., Goodman, M. F., Hanaoka, F., Hinkle, D., Kunkel, T. A., Lawrence, C. W., Livneh, Z., Nohmi, T., Prakash, L., Prakash, S., Todo, T., Walker, G. C., Wang, Z., and Woodgate, R. (2001) *Mol. Cell* **8,** 7–8
6. Yasui, M., Matsui, S., Ihara, M., Laxmi, Y. R., Shibutani, S., and Matsuda, T. (2001) *Nucleic Acids Res.* **29,** 1994–2001
7. Terashima, I., Matsuda, T., Fang, T. W., Suzuki, N., Kobayashi, J., Kohda, K., and Shibutani, S. (2001) *Biochemistry* **40,** 4106–4114
8. Turesky, R. J., and Markovic, J. (1994) *Chem. Res. Toxicol.* **7,** 752–761
9. Meehan, T., and Straub, K. (1979) *Nature* **277,** 410–412
10. Goth, R., and Rajewsky, M. F. (1974) *Proc. Natl. Acad. Sci. U. S. A.* **71,** 639–643
11. Loveless, A. (1969) *Nature* **223,** 206–207
12. Wang, L., Spratt, T. E., Liu, X. K., Hecht, S. S., Pegg, A. E., and Peterson, L. A. (1997) *Chem. Res. Toxicol.* **10,** 562–567
13. Moriya, M., Spiegel, S., Fernandes, A., Amin, S., Liu, T., Geacintov, N., and Grollman, A. P. (1996) *Biochemistry* **35,** 16646–16651
14. Pauly, G. T., Peterson, L. A., and Moschel, R. C. (2002) *Chem. Res. Toxicol.* **15,** 165–169
15. Upton, D. C., Wang, X., Blans, P., Perrino, F. W., Fishbein, J. C., and Akman, S. A. (2006) *Mutat. Res.* **599,** 1–10
16. Upton, D. C., Wang, X., Blans, P., Perrino, F. W., Fishbein, J. C., and Akman, S. A. (2006) *Chem. Res. Toxicol.* **19,** 960–967
17. Choi, J.-Y., and Guengerich, F. P. (2004) *J. Biol. Chem.* **279,** 19217–19229
18. Woodside, A. M., and Guengerich, F. P. (2002) *Biochemistry* **41,** 1027–1038
19. Woodside, A. M., and Guengerich, F. P. (2002) *Biochemistry* **41,** 1039–1050
20. Choi, J.-Y., Angel, K. C., and Guengerich, F. P. (2006) *J. Biol. Chem.* **281,** 21062–21072
21. Choi, J.-Y., and Guengerich, F. P. (2006) *J. Biol. Chem.* **281,** 12315–12324
22. Choi, J.-Y., and Guengerich, F. P. (2005) *J. Mol. Biol.* **352,** 72–90
23. Choi, J.-Y., Chowdhury, G., Zang, H., Angel, K. C., Vu, C. C., Peterson, L. A., and Guengerich, F. P. (2006) *J. Biol. Chem.* **281,** 38244–38256
24. Choi, J.-Y., Stover, J. S., Angel, K. C., Chowdhury, G., Rizzo, C. J., and Guengerich, F. P. (2006) *J. Biol. Chem.* **281,** 25297–25306
25. Choi, J.-Y., Zang, H., Angel, K. C., Kozekov, I. D., Goodenough, A. K., Rizzo, C. J., and Guengerich, F. P. (2006) *Chem. Res. Toxicol.* **19,** 879–886
26. Guo, C., Sonoda, E., Tang, T. S., Parker, J. L., Bielen, A. B., Takeda, S., Ulrich, H. D., and Friedberg, E. C. (2006) *Mol. Cell* **23,** 265–271
27. Guo, C., Tang, T. S., Bienko, M., Parker, J. L., Bielen, A. B., Sonoda, E., Takeda, S., Ulrich, H. D., Dikic, I., and Friedberg, E. C. (2006) *Mol. Cell Biol.* **26,** 8892–8900
28. Guo, C., Fischhaber, P. L., Luk-Paszyc, M. J., Masuda, Y., Zhou, J., Kamiya, K., Kisker, C., and Friedberg, E. C. (2003) *EMBO J.* **22,** 6621–6630
29. Nelson, J. R., Lawrence, C. W., and Hinkle, D. C. (1996) *Nature* **382,** 729–731
30. Zhang, Y., Wu, X., Rechkoblit, O., Geacintov, N. E., Taylor, J. S., and Wang, Z. (2002) *Nucleic Acids Res.* **30,** 1630–1638
31. Guo, D., Xie, Z., Shen, H., Zhao, B., and Wang, Z. (2004) *Nucleic Acids Res.* **32,** 1122–1130
32. Haracska, L., Prakash, S., and Prakash, L. (2002) *J. Biol. Chem.* **277,** 15546–15551
33. Lin, W., Xin, H., Zhang, Y., Wu, X., Yuan, F., and Wang, Z. (1999) *Nucleic Acids Res.* **27,** 4468–4475
34. Nair, D. T., Johnson, R. E., Prakash, L., Prakash, S., and Aggarwal, A. K. (2005) *Science* **309,** 2219–2222
35. Washington, M. T., Minko, I. G., Johnson, R. E., Haracska, L., Harris, T. M., Lloyd, R. S., Prakash, S., and Prakash, L. (2004) *Mol. Cell Biol.* **24,** 6900–6906
36. Borer, P. N. (1975) in *Handbook of Biochemistry and Molecular Biology* (Fasman, G. D., ed) 3rd Ed., pp. 589–590, CRC Press, Inc., Cleveland, OH
37. Pace, C. N., Vajdos, F., Fee, L., Grimsley, G., and Gray, T. (1995) *Protein Sci.* **4,** 2411–2423
38. Goodman, M. F., Creighton, S., Bloom, L. B., and Petruska, J. (1993) *Crit. Rev. Biochem. Mol. Biol.* **28,** 83–126
39. Patel, S. S., Wong, I., and Johnson, K. A. (1991) *Biochemistry* **30,** 511–525
40. Johnson, K. A. (1995) *Methods Enzymol.* **249,** 38–61
41. van Holde, K. E., Johnson, W. C., and Ho, P. S. (1998) *Principles of Physical Biochemistry*, pp. 587–633, Prentice Hall, Upper Saddle River, NJ
42. Herschlag, D., Piccirilli, J. A., and Cech, T. R. (1991) *Biochemistry* **30,** 4844–4854
43. Furge, L. L., and Guengerich, F. P. (1997) *Biochemistry* **36,** 6475–6487
44. Hellman, L. M., and Fried, M. G. (2007) *Nat. Protoc.* **2,** 1849–1861
45. Vaisman, A., Ling, H., Woodgate, R., and Yang, W. (2005) *EMBO J.* **24,** 2957–2967
46. Johnson, K. A. (1993) *Annu. Rev. Biochem.* **62,** 685–713
47. Furge, L. L., and Guengerich, F. P. (1999) *Biochemistry* **38,** 4818–4825
48. Suo, Z., Lippard, S. J., and Johnson, K. A. (1999) *Biochemistry* **38,** 715–726
49. Howell, C. A., Prakash, S., and Washington, M. T. (2007) *Biochemistry* **46,**

13451–13459

50. Washington, M. T., Helquist, S. A., Kool, E. T., Prakash, L., and Prakash, S. (2003) *Mol. Cell Biol.* **23,** 5107–5112
51. Wolfle, W. T., Washington, M. T., Kool, E. T., Spratt, T. E., Helquist, S. A., Prakash, L., and Prakash, S. (2005) *Mol. Cell Biol.* **25,** 7137–7143
52. Eoff, R. L., Irimia, A., Egli, M., and Guengerich, F. P. (2007) *J. Biol. Chem.* **282,** 1456–1467

53. Eoff, R. L., Irimia, A., Angel, K. C., Egli, M., and Guengerich, F. P. (2007) *J. Biol. Chem.* **282,** 19831–19843
54. Johnson, R. E., Prakash, L., and Prakash, S. (2005) *Proc. Natl. Acad. Sci. U. S. A.* **102,** 10466–10471
55. Nair, D. T., Johnson, R. E., Prakash, L., Prakash, S., and Aggarwal, A. K. (2008) *Structure* **16,** 239–245
56. Connolly, M. L. (1993) *J. Mol. Graph.* **11,** 139–141